*Desalination and Water Treatment*
www.deswater.com
doi: 10.1080/19443994.2015.1033651

57 (2016) 10261–10269
May

Taylor & Francis
Taylor & Francis Group

# Adsorption of methylene blue by a low-cost biosorbent: citric acid modified peanut shell

Peng Wang, Qianyun Ma, Dongying Hu, Lijuan Wang*

*Key Laboratory of Bio-based Materials Science and Technology of Ministry of Education, Northeast Forestry University, 26 Hexing Road, Harbin, P.R. China, Tel. +86 18745068285; email: wangpeng8917@126.com (P. Wang), Tel. +86 13091883562; email: maqianyun@126.com (Q. Ma), Tel. +86 15045017413; email: sigl1234@163.com (D. Hu), Tel./Fax: +86 451 82191693; email: donglinwlj@163.com (L. Wang)*

Received 19 September 2014; Accepted 20 March 2015

## ABSTRACT

Peanut shell, an agricultural by-product abundantly available in China, was modified with citric acid and utilized as an adsorbent for the removal of methylene blue (MB) from aqueous solutions. Adsorption studies were conducted to evaluate the effects of pH, contact time, initial dye concentration, and temperature. The kinetic data were analyzed using pseudo-first-order and pseudo-second-order adsorption kinetic models. The results showed that the adsorption process satisfactorily fitted the pseudo-second-order kinetics. The equilibrium data for the adsorption of MB on modified peanut shells were analyzed using the Langmuir and Freundlich models. The results indicate that the Freundlich model provides a better fit of the adsorption data. Thermodynamic parameters such as the changes in Gibbs free energy ($\Delta G^\circ$), enthalpy ($\Delta H^\circ$), and entropy ($\Delta S^\circ$) have also been estimated, and the adsorption process was found to be spontaneous and exothermic. All results demonstrated that peanut shells biomass is an effective adsorbent for removing cationic dyes.

*Keywords:* Adsorption; Citric acid; Methylene blue; Peanut shell

## 1. Introduction

Dyes discharged from textile, printing, and dyeing processes are considered to be one of the most important sources of water pollution. Owing to their synthetic origin and complex aromatic structures, dyes are not easily biodegraded [1]. Several techniques have been used to treat dye-containing effluents, such as sedimentation, chemical treatment, oxidation, electrochemical methodology, biological treatment, adsorption, and ion exchange [2–6]. Among them, adsorption is proved to be an effective and economical process for the removal of pollutants from wastewater. Activated carbon is one of the most commonly used industrial adsorbents because of its high efficiency and wide-ranging availability, but it is too expensive [7]. Hence, there has been increased interest in the use of other adsorbent materials. Recently, a number of studies have been undertaken to investigate the use of low-cost adsorbents, in particular agricultural wastes or by-products such as hazelnut shells, sawdust, maize cob, orange peel, sawdust, rice husk, fly ash, and red mud [8–13].

Peanut is an oil plant that is grown extensively in China. The output of peanuts in China accounts for one-third of the gross production of the world [14].

---

*Corresponding author.

Peanut shell is an abundant and inexpensive agricultural by-product. However, most peanut shells are arbitrarily discarded or set on fire, resulting in environmental pollution and a tremendous waste of natural resources. Recently, there have been several reports that peanut shells can be used as an adsorbent to remove heavy metals, organic pollutants, and dyes from aqueous solution [15–17]. Gonzo et al. synthesized acid-activated carbon from peanut shells for the purpose of removing organic compounds from aqueous solution [18]. Song et al. studied the characteristics of adsorption of methylene blue (MB) by peanut husk in batch and column modes [19]. Chemical modification has often been used to improve adsorption ability. Wafwoyo et al. modified peanut shells (MPS) by treating them with phosphoric and citric acids to increase the metal ion binding ability of the shells [20].

In this work, peanut shell was modified via citric acid treatment to improve the adsorption capacity. The effects of initial dye concentration, pH value, and adsorbent mass on the adsorption process were investigated. The correlations between the experimental data and three kinetic models were examined and the kinetic parameters were determined. The biosorption equilibrium was expressed using the Langmuir and Freundlich isotherms. Finally, thermodynamic parameters were also investigated with respect to temperature.

## 2. Experimental

### 2.1. Preparation of the biosorbent

Peanut shells were purchased from a market of Harbin, China. The collected biomaterial was extensively washed with deionized water to remove soil and dust, and then dried at 80°C to a constant weight to remove moisture and other volatile impurities. The dried sorbent was crushed and milled into a powder, sieved (80–100 mesh), and then stored in a desiccator.

A 1 g sample of powdered peanut shells was mixed with 50 mL of citric acid solution (1 mol $L^{-1}$) and stirred well at 60°C for 2 h. The liquid was discarded and the mixture was filtered, rinsed with distilled water, and oven-dried at 60°C. After 24 h, the temperature was raised to 120°C and held there for 2 h. The modified shells were finally washed in hot water, filtered, and dried in an oven at 60°C for 12 h, then stored prior to adsorption testing.

### 2.2. Characterization of the adsorbents

Fourier transform infrared (FT-IR) spectra of unmodified and MPS were obtained using a Nicolet 560 spectrometer (Nicolet Co., USA) operating in the range of 4,000–400 $cm^{-1}$ with a resolution of 4 $cm^{-1}$ using the KBr pellet method.

### 2.3. Preparation of MB solution

A stock solution of MB (500 mg $L^{-1}$) was prepared in distilled water. All experimental solutions were prepared by diluting the stock solution with distilled water to the required concentration. HCl (1 M) and NaOH (1 M) were used to modify the acidity of the medium.

### 2.4. Adsorption experiments

Batch adsorption experiments were performed in a set of 250 mL flasks containing 100 mg of prepared peanut shells and 50 mL of MB solution. The flasks were shaken in a thermostatted rotary shaker at 120 rpm. At predetermined times, the flasks were withdrawn from the shaker and the residual dye concentration in the reaction mixture was determined using a UV-visible spectrophotometer set at a maximum wavelength of 668 nm. The amount of MB adsorbed per unit weight of adsorbent, $q_t$ (mg $g^{-1}$), was calculated using the following equations:

$$q_t = \frac{(C_0 - C_t)V}{m} \tag{1}$$

where $C_0$ and $C_t$ are the initial and instantaneous concentrations of MB in solution (mg $L^{-1}$), $V$ is the solution volume (L), and $m$ is the mass of the adsorbent (g).

## 3. Results and discussion

### 3.1. FTIR characterization

FT-IR is an important tool for analyzing the functional groups on the surface of the adsorbent material [21]. The FT-IR spectra of natural peanut shells and MPS were obtained and are shown in Fig. 1. In Fig. 1(a), the broad peak around 3,340 $cm^{-1}$ is attributed to the stretching vibration of hydroxyl groups (–OH) from macromolecules such as cellulose, hemicellulose, and lignin. The peak at 2,918 $cm^{-1}$ is assigned to the C–H asymmetrical stretching vibration of methyl groups on the surface. The small peaks at 1,730 and 1,622 $cm^{-1}$ are characteristic of carbonyl group stretching in carboxylic acids and carbonyl groups. The band at 1,507 $cm^{-1}$ is associated with stretching of aromatic rings. The peak at 1,423 $cm^{-1}$ is caused by $CH_2$ bending and the peak at

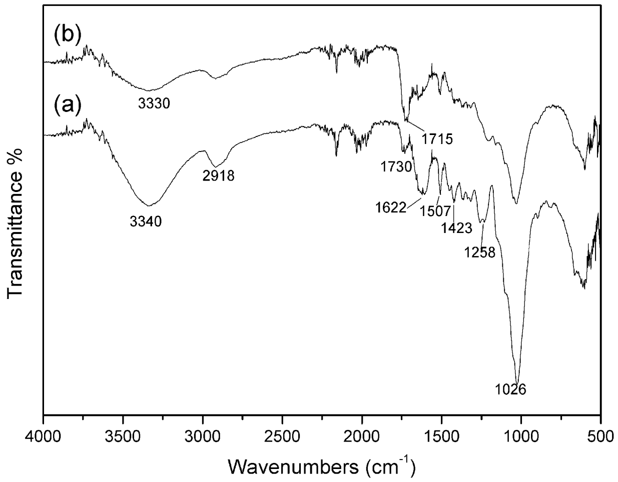

Fig. 1. FT-IR spectra of the peanut shell before (a) and after (b) modification.

$1,258\ cm^{-1}$ is indicative of OH in-plane bending in cellulose. The sharp peak at $1,026\ cm^{-1}$ is due to the C–O group in carboxylic and alcoholic groups [19]. The spectra of MPS showed characteristics that are similar to those of the natural peanut shells except for slight changes. After modification, the intensity of the band at $1,026\ cm^{-1}$ decreased, and the peak at $3,340\ cm^{-1}$ decreased and shifted to $3,330\ cm^{-1}$. However, the intensity of the carboxyl group at $1,730\ cm^{-1}$ increased significantly. It obviously was due to the carboxyl groups of the introduced citric acid [22]. This result indicated that the peanut shells were successfully modified by citric acid. Fig. 2 shows a schematic representation of the possible interactions between the MB molecules and the adsorbent structure.

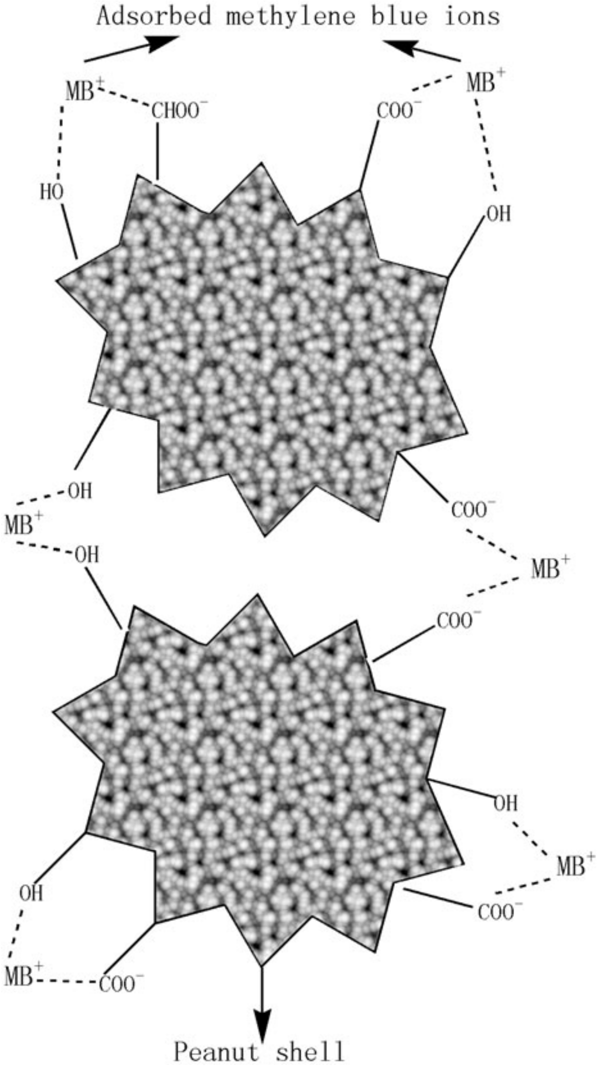

Fig. 2. Schematic diagram of the adsorption of MB molecules on MPS.

### 3.2. Effect of initial pH

The pH is one of the most important factors controlling the adsorption of a dye onto suspended particles. The effect of pH on MB adsorption is shown in Fig. 3(a). It appears that the removal rate of MB by MPS increased from 64.5 to 95.6% with an increase in pH from 2 to 10. This behavior can be explained on the basis of the point of zero charge ($pH_{zpc}$) of the adsorbent. Fig. 3(b) shows that the $pH_{zpc}$ of MPS was around 2.6, which means that the MPS surface was more positively charged when the dye solution pH was lower than 2.6 and negatively charged at a pH higher than 2.6. Theoretically, at a pH lower than $pH_{zpc}$, the number of negatively charged adsorbent sites decreases and the number of positively charged surface sites increases, which does not favor the adsorption of MB (a cationic dye) due to electrostatic repulsion. As the pH of the solution increased past the $pH_{zpc}$, the net charge on the surface of the MPS became negative, which enhances the electrostatic interaction between the cationic MB species and the negatively charged adsorbent surface [23,24]. The electrostatic attractive force between the dye compound and the peanut shell surface is likely to be greater when the pH increases. This strong chelating interaction accounts for the higher removal efficiency of the biosorbent.

### 3.3. Effect of initial dye concentration

The effect on adsorption when the initial dye concentration varied in the range of 60–120 $mg\ L^{-1}$

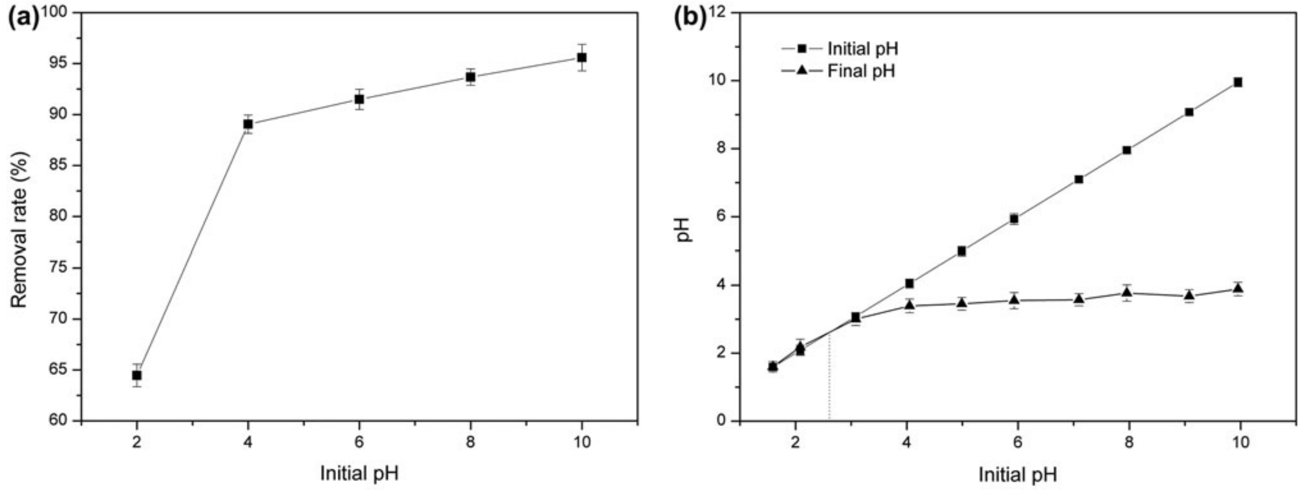

Fig. 3. Effects of initial solution pH (a) and final pH (b) on the adsorption of MB (loading 100 mg, $C = 100\ \mathrm{mg\ L^{-1}}$, $V = 50$ mL, $t = 720$ min, and $T = 303$ K).

was investigated and is shown in Fig. 4. The amount of dye adsorbed increased from 28.2 to 52.1 $\mathrm{mg\ g^{-1}}$ when the initial concentration of MB dye increased from 60 to 120 $\mathrm{mg\ L^{-1}}$. This is because the initial dye concentration provides the necessary driving force to overcome the resistance to mass transfer of the dye molecules between the aqueous phase and the solid phase [25]. An increase in the initial dye concentration also enhances the interaction between MB and the peanut shells. Therefore, an increase in initial MB concentration leads to an increase in the adsorption uptake of MB. It is also found from Fig. 4 that the equilibrium time increased with the increase of dye concentration. This can be explained by the theory that the molecules have to penetrate the boundary layer before the dye molecules successfully diffused and adsorbed on the adsorbent surface. Besides, the agglomeration of MB may occur at high MB concentration which would also slow down the adsorption process. Therefore, higher concentration of MB will require more time to attain equilibrium [26].

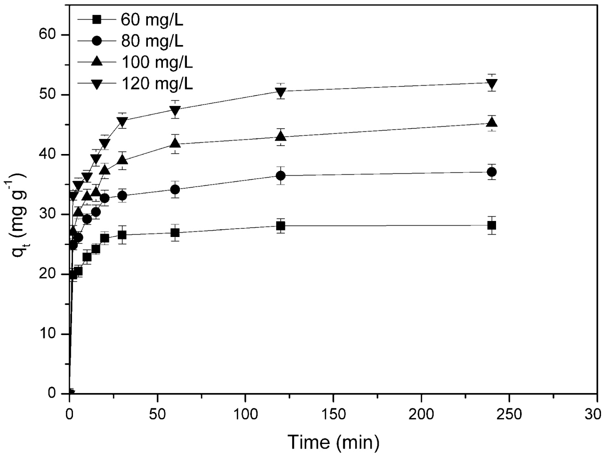

Fig. 4. Effects of initial solution concentration on the adsorption of MB onto MPS (loading 100 mg, $V = 50$ mL, and $T = 303$ K).

### 3.4. Adsorption kinetics

The kinetic parameters are helpful for predicting the dominant adsorption mechanism and the adsorption rate of the adsorbent, which provides important information about the efficiency of the adsorption [27]. To investigate the adsorption kinetics of MB on MPS, three different kinetic models, namely the Lagergren pseudo-first-order, pseudo-second-order, and intra-particle diffusion kinetic equations were used to test the experimental data. The pseudo-first-order kinetic model was suggested by Lagergren for adsorption in solid/liquid systems and its formula can be expressed as [28]:

$$\ln\,(q_e - q_t) = \ln\ q_e - k_1 t \tag{2}$$

where $q_e$ and $q_t$ are the amounts of MB ($\mathrm{mg\ g^{-1}}$) adsorbed on the adsorbent at equilibrium and at a given time $t$ (min), respectively; $k_1$ is the rate constant (1/min) of the Lagergren first-order kinetic model. Values of $k_1$ are calculated by plotting ln ($q_e$–$q_t$) vs. $t$.

The pseudo-second-order kinetic model is expressed as [29]:

$$\frac{t}{q_t} = \frac{1}{k_2 q_e^2} + \frac{t}{q_e} \quad (3)$$

where $k_2$ is the rate constant of pseudo-second-order adsorption (g mg$^{-1}$ min$^{-1}$). Values of $k_2$ are obtained by plotting $(t/q_t)$ vs. $t$.

The linear forms of the two models for the adsorption of MB onto MPS at 303 K are shown in Fig. 5 and the kinetic parameters and correlation coefficients are summarized in Table 1. For all experimental initial dye concentrations, the values of the linear correlation coefficient of the pseudo-second-order model are very high (>0.999). In addition, the values of the calculated equilibrium adsorption capacity also agree well with the experimental data. Therefore, the pseudo-second-order kinetic model is more valid for this adsorption process than the pseudo-first-order model. This suggests that chemical sorption is the rate-limiting step of the adsorption mechanism, and that mass transfer in the solution is not involved [30]. Also from Table 1, the values of the rate constant, $k_2$, decrease with initial dye concentration for peanut shells. The reason for this behavior is that there is less competition for sorption sites at lower concentrations. At higher concentrations, the competition for surface active sites will be high and, consequently, low sorption rates are obtained.

Most adsorption processes consist of multiple steps, including surface diffusion and intraparticle diffusion. To determine whether intraparticle diffusion is the rate-determining step, the intraparticle mass-transfer diffusion model is applied. It can be expressed as [31]:

$$q_t = k_{id} t^{1/2} + c \quad (4)$$

where $c$ is the intercept (mg g$^{-1}$) and $k_{id}$ is the intraparticle diffusion rate constant (mg g$^{-1}$ min$^{-1/2}$), which can be calculated from the slope of the linear plot of $q_t$ vs. $t^{1/2}$ as shown in Fig. 6. The adsorption process tends to have two phases: the initial curved portion and a second linear portion. The curve of the first portion of the plot is the result of surface adsorption and external diffusion, indicating a boundary-layer effect, whereas the linear portion reflects intraparticle or pore diffusion. The linear portions of the curves at each concentration do not pass through the origin, suggesting that intraparticle diffusion is not the sole rate-limiting step [30]. In addition, the intercept value decreases with increasing initial MB concentration, indicating a decrease in the thickness of the boundary layer and its effect on adsorption.

## 3.5. Adsorption isotherms

Adsorption isotherm models can describe the interaction between an adsorbent and the given adsorbate, which is a critical factor in optimizing the use of adsorbents. The adsorption of MB onto MPS was carried out at adsorbent loading ranging from 75 to 200 mg. The adsorption isotherm experimental data were fitted by two well-known adsorption isotherms models: those of Langmuir [32] and Freundlich [33]. The Langmuir (Eq. (5)) and Freundlich (Eq. (6)) isotherms can be expressed as follows:

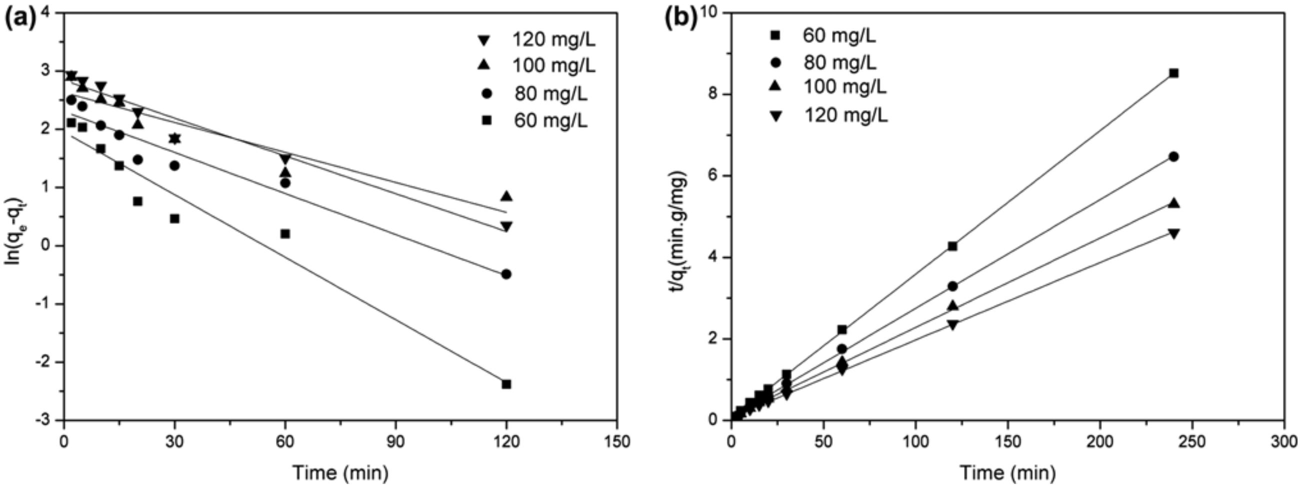

Fig. 5. Lagergren first-order kinetic model (a) and pseudo-second-order kinetic model (b) for adsorption of MB onto MPS at 303 K.

Table 1
Kinetic parameters for MB adsorption onto MPS

| | | Lagergren pseudo-first-order model | | | Pseudo-second-order model | | |
|---|---|---|---|---|---|---|---|
| $C_0$ (mg $L^{-1}$) | $q_{e,\text{exp}}$ (mg $g^{-1}$) | $q_{1e,\text{cal}}$ (mg $g^{-1}$) | $k_1 \times 10^3$ ($\text{min}^{-1}$) | $R^2$ | $q_{2e,\text{cal}}$ (mg $g^{-1}$) | $k_2 \times 10^3$ (g $\text{mg}^{-1}$ $\text{min}^{-1}$) | $R^2$ |
| 60 | 28.17 | 7.04 | 35.80 | 0.9538 | 28.41 | 17.28 | 0.9999 |
| 80 | 37.11 | 10.04 | 23.50 | 0.9508 | 37.45 | 8.78 | 0.9999 |
| 100 | 45.23 | 13.87 | 17.10 | 0.8777 | 45.66 | 5.20 | 0.9997 |
| 120 | 52.03 | 17.11 | 21.60 | 0.9654 | 52.63 | 4.59 | 0.9991 |

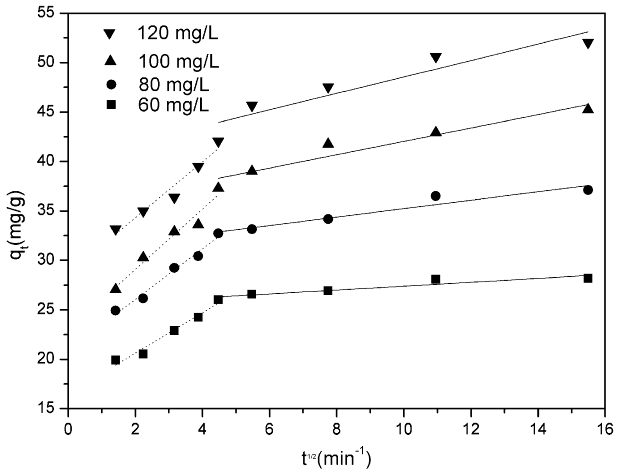

Fig. 6. The intraparticle diffusion kinetic model for adsorption of MB onto MPS at 303 K.

$$\frac{C_e}{q_e} = \frac{1}{K_L q_m} + \frac{C_e}{q_m} \tag{5}$$

$$\ln\, q_e = \ln\, K_F + \left(\frac{1}{n}\right) \ln\, C_e \tag{6}$$

where $C_e$ is the equilibrium concentration of MB in solution (mg $L^{-1}$); $q_e$ is the amount of MB adsorbed at equilibrium (mg $g^{-1}$); $q_m$ is the maximum adsorption capacity; $K_L$ is the Langmuir adsorption constant, which is related to the energy of adsorption (L $\text{mg}^{-1}$); and $K_F$ and $n$ are the Freundlich constants related to the adsorption capacity and the surface heterogeneity, respectively.

The slope and intercept of linear plots of $C_e/q_e$ against $C_e$ yield the values of $1/q_m$ and $1/K_L q_m$ for Eq. (5), and the slope and intercept of linear plots of $\ln q_e$ against $\ln C_e$ yield the values of $1/n$ and $\ln K_F$ for Eq. (6). The theoretical parameters of adsorption isotherms along with the correlation coefficients ($R^2$) are given in Table 2. The Langmuir isotherm is valid for the adsorption of a solute from a liquid solution when it corresponds to monolayer adsorption on a surface containing a finite number of identical sites. In contrast, the Freundlich isotherm model is valid for multilayer adsorption and is derived by assuming a heterogeneous surface with interactions between adsorbed molecules with a non-uniform distribution of heat of sorption over the surface. The Freundlich constant $K_F$ is indicative of the adsorption capacity of the adsorbent: the greater the $K_F$ value, the greater the adsorption capacity. The other Freundlich constant $n$ is a measure of the deviation from linearity of the adsorption and is used to verify the types of adsorption. It is suggested that, if $n$ is equal to unity, the adsorption is linear. Further, $n$ values below unity indicate that adsorption is a chemical process, whereas, $n$ values above unity are associated with favorable adsorption and a physical process [34]. As indicated by the correlation coefficients, $R^2$, the adsorption processes were better described by the Freundlich isotherm model. The value of $n$ is larger than 1, which indicates the favorable nature of adsorption and a physical process.

Table 3 list the comparison of maximum monolayer adsorption capacity of MB using various adsorbents. The results show that MPS is an effective adsorbent for MB.

### 3.6. Thermodynamic parameters

It is well known that the values of thermodynamic parameters such as the Gibbs free energy change ($\Delta G^\circ$), enthalpy change ($\Delta H^\circ$), and entropy change ($\Delta S^\circ$) must be taken into consideration in order to evaluate the spontaneity of the adsorption process. Experiments were performed at different temperatures (303, 313, 323, and 333 K) to investigate the effect of temperature, with an initial MB concentration of 100 mg $L^{-1}$ and an adsorbent loading of 100 mg. The thermodynamic parameters can be calculated according to the following Van't Hoff equation [47]:

$$\Delta G^\circ = \Delta H^\circ - T\Delta S^\circ = -RT \ln K_c \tag{7}$$

Table 2
Langmuir and Freundlich isotherm constants at different temperatures

| | Langmuir isotherm constants | | | Freundlich isotherm constants | | |
|---|---|---|---|---|---|---|
| $T$ (K) | $q_m$ (mg $g^{-1}$) | $K_L$ | $R^2$ | $K_F$ ($mg^{1-(1/n)}$ $L^{1/n}$ $g^{-1}$) | $n$ | $R^2$ |
| 303 | 120.48 | 0.069 | 0.9643 | 10.32 | 1.48 | 0.9733 |
| 313 | 119.05 | 0.061 | 0.9444 | 9.55 | 1.47 | 0.9803 |
| 323 | 108.69 | 0.043 | 0.8811 | 7.48 | 1.57 | 0.9834 |

Table 3
Comparison of maximum adsorption capacity ($q_{\max}$) of different adsorbents towards MB

| Adsorbent | $q_{\max}$ (mg $g^{-1}$) | References |
|---|---|---|
| Kenaf core fibers | 131.6 | [35] |
| Rejected tea | 156 | [36] |
| Meranti sawdust | 158.73 | [37] |
| Mango seed kernel powder | 153.85 | [38] |
| Poplar sawdust | 153 | [39] |
| Garlic peel | 142.86 | [40] |
| Jute processing water | 22.47 | [41] |
| Wheat shells | 16.56 | [42] |
| Rice husk | 40.6 | [43] |
| Hazelnut | 76.9 | [44] |
| Cherry sawdust | 39.84 | [44] |
| Oak sawdust | 29.94 | [44] |
| Coir pith carbon | 5.87 | [45] |
| Waste apricot-based activated carbon | 102.04–136.98 | [46] |
| MPS | 120.48 | This work |

$$K_c = \frac{C_s}{C_e} \tag{8}$$

$$\ln K_c = \frac{\Delta S^\circ}{R} - \frac{\Delta H^\circ}{RT} \tag{9}$$

where $\Delta G^\circ$ (kJ $mol^{-1}$), $\Delta H^\circ$ (kJ $mol^{-1}$), and $\Delta S^\circ$ (J $mol^{-1}$ $K^{-1}$) are the changes in Gibbs free energy, enthalpy, and entropy, respectively; $R$ is the ideal gas constant (8.314 J $mol^{-1}$ $K^{-1}$); $T$ is the absolute temperature (K); $K_c$, the equilibrium constant, is the ratio of the concentration of MB on the adsorbent at equilibrium ($C_s$) to the remaining concentration of the dye in solution at equilibrium ($C_e$).

Plotting ln $K_c$ against $1/T$ gives a straight line from which $\Delta H^\circ$ and $\Delta S^\circ$ are calculated from the slope and intercept, respectively. The values of $\Delta G^\circ$, $\Delta H^\circ$, and $\Delta S^\circ$ are listed in Table 4. The negative $\Delta H^\circ$ value confirms that the adsorption processes are exothermic in nature. The negative $\Delta G^\circ$ implies the spontaneity of the adsorption. The observed decrease in negative values of $\Delta G^\circ$ with increasing temperature implies that the adsorption becomes less favorable at higher temperatures. The negative value of $\Delta S^\circ$ suggests a

Table 4
Thermodynamic parameters for the adsorption of MB onto MP

| $T$ (K) | $\Delta G^\circ$ (kJ $mol^{-1}$) | $T\Delta S^\circ$ (kJ $mol^{-1}$) | $\Delta H^\circ$ (kJ $mol^{-1}$) | $\Delta S^\circ$ (J $mol^{-1}$ $K^{-1}$) |
|---|---|---|---|---|
| 303 | −6.073 | −18.266 | −24.339 | −60.2856 |
| 313 | −5.470 | −18.869 | | |
| 323 | −4.867 | −19.472 | | |
| 333 | −4.264 | −20.075 | | |

decrease in randomness at the solid/solution interface during the adsorption of MB onto peanut shells.

## 4. Conclusions

An effective biosorbent was prepared from peanut shells by treatment with citric acid. The adsorption of MB onto MPS was studied as a function of the pH of the aqueous solution and the initial dye concentration. The amounts of MB adsorbed increased with increasing pH value and initial dye concentration. The kinetic data were analyzed using pseudo-first-order and pseudo-second-order adsorption kinetic models. The results indicated that the pseudo-second-order equation provides the better correlation with the adsorption data. Isotherm data were treated according to the Langmuir and Freundlich models; the Freundlich isotherm model provided a better fit compared to the Langmuir model in the temperature range studied. The thermodynamic constants of adsorption were also evaluated and the process was found to be spontaneous and exothermic.

## Acknowledgments

The authors gratefully acknowledge support from the Fundamental Research Funds for the Central Universities (DL12DB04).

## References

[1] M.T. Yagub, T.K. Sen, S. Afroze, H.M. Ang, Dye and its removal from aqueous solution by adsorption: A review, Adv. Colloid Interface Sci. 209 (2014) 172–184.

[2] V.K. Gupta, Suhas, Application of low-cost adsorbents for dye removal—A review, J. Environ. Manage. 90 (2009) 2313–2342.

[3] A. Mishra, M. Bajpai, The flocculation performance of *Tamarindus* mucilage in relation to removal of vat and direct dyes, Bioresour. Technol. 97 (2006) 1055–1059.

[4] X. Zhou, Y. Li, Y. Zhao, Removal characteristics of organics and nitrogen in a novel four-stage biofilm integrated system for enhanced treatment of coking wastewater under different HRTs, RSC Advances 4 (2014) 15620–15629.

[5] J.R. Steter, W.R. Barros, M.R. Lanza, A.J. Motheo, Electrochemical and sonoelectrochemical processes applied to amaranth dye degradation, Chemosphere 117 (2014) 200–207.

[6] C.H. Liu, J.S. Wu, H.C. Chiu, S.Y. Suen, K.H. Chu, Removal of anionic reactive dyes from water using anion exchange membranes as adsorbers, Water Res. 41 (2007) 1491–1500.

[7] G. Crini, Non-conventional low-cost adsorbents for dye removal: A review, Bioresour. Technol. 97 (2006) 1061–1085.

[8] I. Ali, M. Asim, T.A. Khan, Low cost adsorbents for the removal of organic pollutants from wastewater, J. Environ. Manage. 113 (2012) 170–183.

[9] C. Djilani, R. Zaghdoudi, A. Modarressi, M. Rogalski, F. Djazi, A. Lallam, Elimination of organic micropollutants by adsorption on activated carbon prepared from agricultural waste, Chem. Eng. J. 189–190 (2012) 203–212.

[10] D. Kalderis, D. Koutoulakis, P. Paraskeva, E. Diamadopoulos, E. Otal, J.O.d. Valle, C. Fernández-Pereira, Adsorption of polluting substances on activated carbons prepared from rice husk and sugarcane bagasse, Chem. Eng. J. 144 (2008) 42–50.

[11] M.K. Sahu, S. Mandal, S.S. Dash, P. Badhai, R.K. Patel, Removal of Pb(II) from aqueous solution by acid activated red mud, J. Environ. Chem. Eng. 1 (2013) 1315–1324.

[12] S. Wang, Y. Boyjoo, A. Choueib, Z.H. Zhu, Removal of dyes from aqueous solution using fly ash and red mud, Water Res. 39 (2005) 129–138.

[13] R. Sivaraj, C. Namasivayam, K. Kadirvelu, Orange peel as an adsorbent in the removal of Acid violet 17 (acid dye) from aqueous solutions, Waste Manage. 21 (2001) 105–110.

[14] Z.Y. Zhong, Q. Yang, X.M. Li, K. Luo, Y. Liu, G.M. Zeng, Preparation of peanut hull-based activated carbon by microwave-induced phosphoric acid activation and its application in Remazol Brilliant Blue R adsorption, Ind. Crops Prod. 37 (2012) 178–185.

[15] A. Witek-Krowiak, R.G. Szafran, S. Modelski, Biosorption of heavy metals from aqueous solutions onto peanut shell as a low-cost biosorbent, Desalination 265 (2011) 126–134.

[16] R. Gong, M. Li, C. Yang, Y. Sun, J. Chen, Removal of cationic dyes from aqueous solution by adsorption on peanut hull, Removal of cationic dyes from aqueous solution by adsorption on peanut hull, J. Hazard. Mater. 121 (2005) 247–250.

[17] M.Ş. Tanyildizi, Modeling of adsorption isotherms and kinetics of reactive dye from aqueous solution by peanut hull, Chem. Eng. J. 168 (2011) 1234–1240.

[18] E.E. Gonzo, A. Bonomo, L.C. Romero, Acid-activated carbons from peanut shells: Synthesis, characterization and uptake of organic compounds from aqueous solutions, Adsorpt. Sci. Technol. 21 (2003) 617–626.

[19] J. Song, W. Zou, Y. Bian, F. Su, R. Han, Adsorption characteristics of methylene blue by peanut husk in batch and column modes, Desalination 265 (2011) 119–125.

[20] W. Wafwoyo, C.W. Seo, W.E. Marshall, Utilization of peanut shells as adsorbents for selected metals, J. Chem. Technol. Biotechnol. 74 (1999) 1117–1121.

[21] R. Han, L. Zhang, C. Song, M. Zhang, H. Zhu, L. Zhang, Characterization of modified wheat straw, kinetic and equilibrium study about copper ion and methylene blue adsorption in batch mode, Carbohydr. Polym. 79 (2010) 1140–1149.

[22] R. Gong, K. Zhong, Y. Hu, J. Chen, G. Zhu, Thermochemical esterifying citric acid onto lignocellulose for enhancing methylene blue sorption capacity of rice straw, J. Environ. Manage. 88 (2008) 875–880.

[23] M. Dogan, H. Abak, M. Alkan, Adsorption of methylene blue onto hazelnut shell: Kinetics, mechanism and activation parameters, J. Hazard. Mater. 164 (2009) 172–181.

[24] S. Jain, R.V. Jayaram, Removal of basic dyes from aqueous solution by low-cost adsorbent: Wood apple shell (*Feronia acidissima*), Desalination 250 (2010) 921–927.

[25] P. Senthil Kumar, S. Ramalingam, C. Senthamarai, M. Niranjanaa, P. Vijayalakshmi, S. Sivanesan, Adsorption of dye from aqueous solution by cashew nut shell: Studies on equilibrium isotherm, kinetics and thermodynamics of interactions, Desalination 261 (2010) 52–60.

[26] I.A.W. Tan, A.L. Ahmad, B.H. Hameed, Adsorption of basic dye on high-surface-area activated carbon prepared from coconut husk: Equilibrium, kinetic and thermodynamic studies, J. Hazard. Mater. 154 (2008) 337–346.

[27] H.Y. Zhu, Y.Q. Fu, R. Jiang, J. Yao, L. Xiao, G.M. Zeng, Novel magnetic chitosan/poly(vinyl alcohol) hydrogel beads: Preparation, characterization and application for adsorption of dye from aqueous solution, Bioresour. Technol. 105 (2012) 24–30.

[28] Y.S. Ho, G. McKay, A comparison of chemisorption kinetic models applied to pollutant removal on various sorbents, Process Saf. Environ. Prot. 76 (1998) 332–340.

[29] Y.S. Ho, G. McKay, Pseudo-second order model for sorption processes, Process Biochem. 34 (1999) 451–465.

[30] H.Y. Zhu, R. Jiang, L. Xiao, W. Li, A novel magnetically separable $\gamma$-$Fe_2O_3$/crosslinked chitosan adsorbent: Preparation, characterization and adsorption application for removal of hazardous azo dye, J. Hazard. Mater. 179 (2010) 251–257.

[31] W. Weber, J. Morris, Kinetics of adsorption on carbon from solution, J. Sanit. Eng. Div. Am. Soc. Civ. Eng. 89 (1963) 31–60.

[32] I. Langmuir, The adsorption of gases on plane surfaces of glass, mica and platinum, J. Am. Chem. Soc. 40 (1918) 1361–1403.

[33] H. Freundlich, Of the adsorption of gases. Section II. Kinetics and energetics of gas adsorption. Introductory paper to section II, Trans. Faraday Soc. 28 (1932) 195–201.

[34] S. Dawood, T.K. Sen, Removal of anionic dye Congo red from aqueous solution by raw pine and acid-treated pine cone powder as adsorbent: Equilibrium, thermodynamic, kinetics, mechanism and process design, Water Res. 46 (2012) 1933–1946.

[35] M.S. Sajab, C.H. Chia, S. Zakaria, S.M. Jani, M.K. Ayob, K.L. Chee, P.S. Khiew, W.S. Chiu, Citric acid modified kenaf core fibres for removal of methylene blue from aqueous solution, Bioresour. Technol. 102 (2011) 7237–7243.

[36] N. Nasuha, B.H. Hameed, A.T. Din, Rejected tea as a potential low-cost adsorbent for the removal of methylene blue, J. Hazard. Mater. 175 (2010) 126–132.

[37] A. Ahmad, M. Rafatullah, O. Sulaiman, M.H. Ibrahim, R. Hashim, Scavenging behaviour of meranti sawdust in the removal of methylene blue from aqueous solution, J. Hazard. Mater. 170 (2009) 357–365.

[38] K.V. Kumar, A. Kumaran, Removal of methylene blue by mango seed kernel powder, Biochem. Eng. J. 27 (2005) 83–93.

[39] H. Pekkuz, I. Uzun, F. Guzel, Kinetics and thermodynamics of the adsorption of some dyestuffs from aqueous solution by poplar sawdust, Bioresour. Technol. 99 (2008) 2009–2017.

[40] B.H. Hameed, A.A. Ahmad, Batch adsorption of methylene blue from aqueous solution by garlic peel, an agricultural waste biomass, J. Hazard. Mater. 164 (2009) 870–875.

[41] S. Banerjee, M.G. Dastidar, Use of jute processing wastes for treatment of wastewater contaminated with dye and other organics, Bioresour. Technol. 96 (2005) 1919–1928.

[42] Y. Bulut, H. Aydın, A kinetics and thermodynamics study of methylene blue adsorption on wheat shells, Desalination 194 (2006) 259–267.

[43] V. Vadivelan, K.V. Kumar, Equilibrium, kinetics, mechanism, and process design for the sorption of methylene blue onto rice husk, J. Colloid Interface Sci. 286 (2005) 90–100.

[44] F. Ferrero, Dye removal by low cost adsorbents: Hazelnut shells in comparison with wood sawdust, J. Hazard. Mater. 142 (2007) 144–152.

[45] D. Kavitha, C. Namasivayam, Experimental and kinetic studies on methylene blue adsorption by coir pith carbon, Bioresour. Technol. 98 (2007) 14–21.

[46] C.A. Basar, Applicability of the various adsorption models of three dyes adsorption onto activated carbon prepared waste apricot, J. Hazard. Mater. 135 (2006) 232–241.

[47] J. Tellinghuisen, Van't Hoff analysis of K degrees (T): how good...or bad? Biophys. Chem. 120 (2006) 114–120.